

## Visualization of Small Ordered Domains in a Matrix of Disordered Ferroelectric Oxides by Electron Microscopy Structure Imaging

G. NIHOUL AND M. H. PISCHEDDA

*Laboratoire Matériaux Multiphasés et Interfaces, Université de Toulon et du Var, BP 132, 83957 La Garde Cedex, France*

Received June 29, 1992; in revised form November 9, 1992; accepted November 11, 1992

In a previous paper, we have shown that high resolution electron microscopy (HREM) is able to reveal nanometric domains in ferroelectric oxides, the existence of which cannot be proven by other means. However, this method cannot reveal all the domains. In this paper we calculate the limits of the HREM possibilities and expound a method to obtain some statistical information on the observed sample. © 1993 Academic Press, Inc.

### 1. Introduction

Ferroelectric mixed lead oxides, such as  $\text{Pb}_2\text{ScTaO}_6$  and  $\text{Pb}_2\text{ScNbO}_6$ , have interesting properties (1-5), in particular a broad dielectric permittivity peak vs temperature and dielectric dispersion at low frequencies. Most of these properties are linked with a disordered structure where the cations, other than lead, are randomly distributed among their sites (6-8). Their properties are changed when ordered domains exist in the specimen (9, 10). However, other reasons could also explain these modified properties and it is thus important to prove the existence of these ordered domains in a disordered matrix. X-Ray experiments provide some indications, but the lines due to the ordered part are very weak, especially because of the strong absorption due to lead. A certain number of electron microscopy studies have been carried out (11, 12). Bright field electron microscopy is of no help, as the transmitted intensities for both ordered or disordered phases are closely similar, though this method has been successfully used to reveal the ferroelectric domain boundaries (13, 14). Dark field electron microscopy,

using a diffracted beam occurring only for the ordered phase, does show the existence of ordered domains but will not reveal small domains (smaller than 4 nm) which are believed to exist. Thus, the only possibility for visualizing small domains is high resolution electron microscopy (HREM), where both transmitted and diffracted beams are included. In a previous paper (15), we demonstrated that this technique indeed reveals small domains if one uses small spatial frequencies; in this case, the HREM image for a disordered structure is very different from the one observed for an ordered structure. Another HREM study carried out on PSN and PST shows some structure which could be interpreted as ordered domains (16); however, the question of the real size of these domains is difficult to answer. Figure 1 shows an example of an experimental image, with fringes, and some areas where a spot pattern can be seen. In this paper, we attempt to interpret such an image by examining a small ordered cluster in a disordered matrix to see if very small clusters can be seen, even in a thick matrix, and to determine under what experimental conditions this can be achieved.

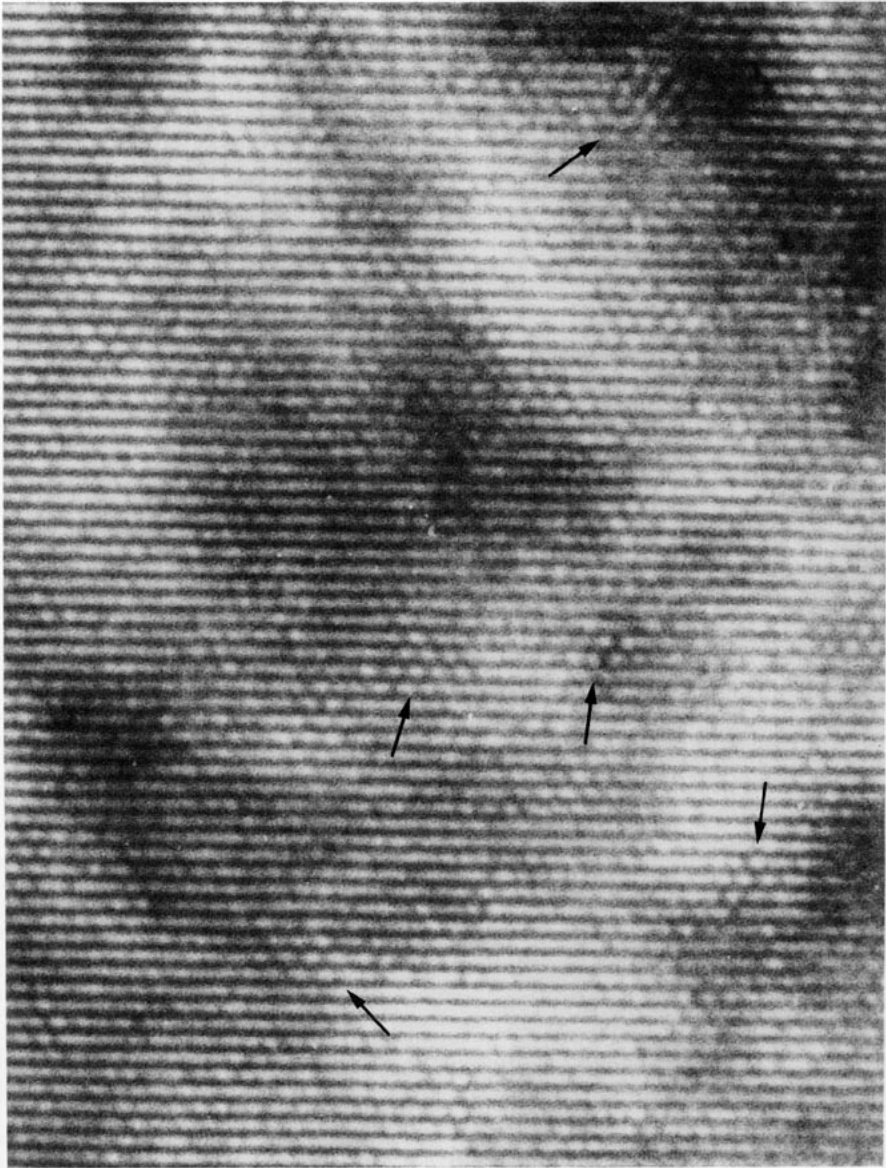


FIG. 1. Experimental high resolution electron microscopy image of an PSN crystallite. One can see some disordered regions (fringes) and some areas with a pattern of spots which we want to interpret as being ordered regions. (By courtesy of Q. Li and J. G. Zheng.)

## 2. Model and Computation

These oxides have a perovskite-type structure where lead atoms occupy the A sites and the two other cations occupy the B and B' sites. Figure 2 shows the structure for the ordered perovskite, where the cubic cell parameter is 0.814 nm, and for the disor-

dered structure, which can be described by a cubic cell of half the parameter. For simplicity, all calculations and discussions are done using the same large cell. Disordered permitted reflections must then have all their indices even, with no other selection rule, while the ordered structure, having fcc translations, give rise to reflections with a

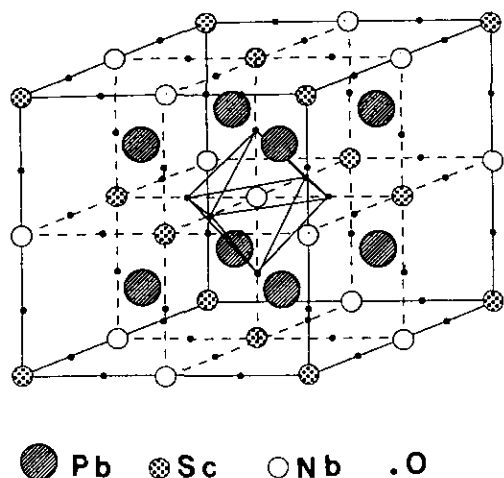


FIG. 2. Structure of the ordered perovskite  $\text{Pb}_2\text{ScNbO}_6$ , with the different atoms shown (after Galasso, Ref. (6)).

nonzero structure factor only if their indices have the same parity. This means that all reflections with three odd indices can exist, but only in the ordered structure, while reflections with three even indices can exist in both structures. Therefore, it is not of interest to carry out HREM studies with an electron beam parallel to the  $[111]$  direction (reflections with  $h + k + l = 0$ ) or the  $[100]$  direction (reflections with  $h = 0$ ) where only planes with even indices (common to both structures) diffract, as no difference will be noted between the two structures. In real space, this corresponds to a situation where the projected planes all contain the same number of cations, so that it makes no difference whether or not they are randomly distributed in these planes. Only  $[110]$  HREM images indicate a difference between ordered and disordered domains. Figure 3 shows a drawing of the diffraction pattern obtained along the  $[110]$  axis, as well as an experimental pattern. Images obtained by interference between the transmitted beam, the  $(111)$  diffracted beams, and the  $(002)$  beams are very different according to the corresponding structure: for a disordered structure (where the  $(111)$  beams are forbidden, even by double diffraction), we obtain

a fringe image, with fringes parallel to the  $(002)$  planes. For an ordered structure, we have an interference image between the transmitted beam and six diffracted beams, which produce a spot image, with an irregular hexagonal pattern, for suitable imaging conditions. These are the conditions we want to determine, taking into account the thickness of the sample (ordered and disordered portions), the imaging defocus, and the size of the ordered cluster. The reticular distances corresponding to these planes are rather large (0.433 nm for the  $(111)$  planes and 0.400 nm for the  $(002)$  planes). It is not useful to try to achieve better resolution by taking more diffracted beams: the pattern due to the disordered matrix also becomes a spot pattern, more intricate than a simple fringe pattern. Any ordered inclusion only gives rise to a small alteration of this pattern, which can be detected only with difficulty. On the other hand, the difference between a fringe pattern and a spot pattern is easily recognized.

We first tested the influence of thickness and of imaging defocus on a model where the ordered inclusion has a constant thickness, i.e., has boundaries parallel to the incident beam (direction  $[110]$ ). We consider an inclusion with boundaries parallel to the  $(001)$  and  $(110)$  planes, with lateral dimensions 1.63 and 2.2 nm, which, laterally, corresponds roughly to two basic cells. We tried two thicknesses for the inclusion, 2.2 and 3 nm. The matrix thickness ranges from 5 to 18 nm, which corresponds to the range of thicknesses used for HREM.

We then tested very small inclusions with nonconstant thickness to establish whether they could be detected and what they would look like. For this purpose, a single unit cell inclusion, with boundaries parallel to  $(100)$  planes, was embedded in a disordered matrix and rotated so as to be observed along a  $[110]$  axis; along this direction, the inclusion has variable thickness. Again, we calculated what would be observed for different matrix thicknesses and imaging defocus.

The computations were performed using the "multislice" method (17) to describe the

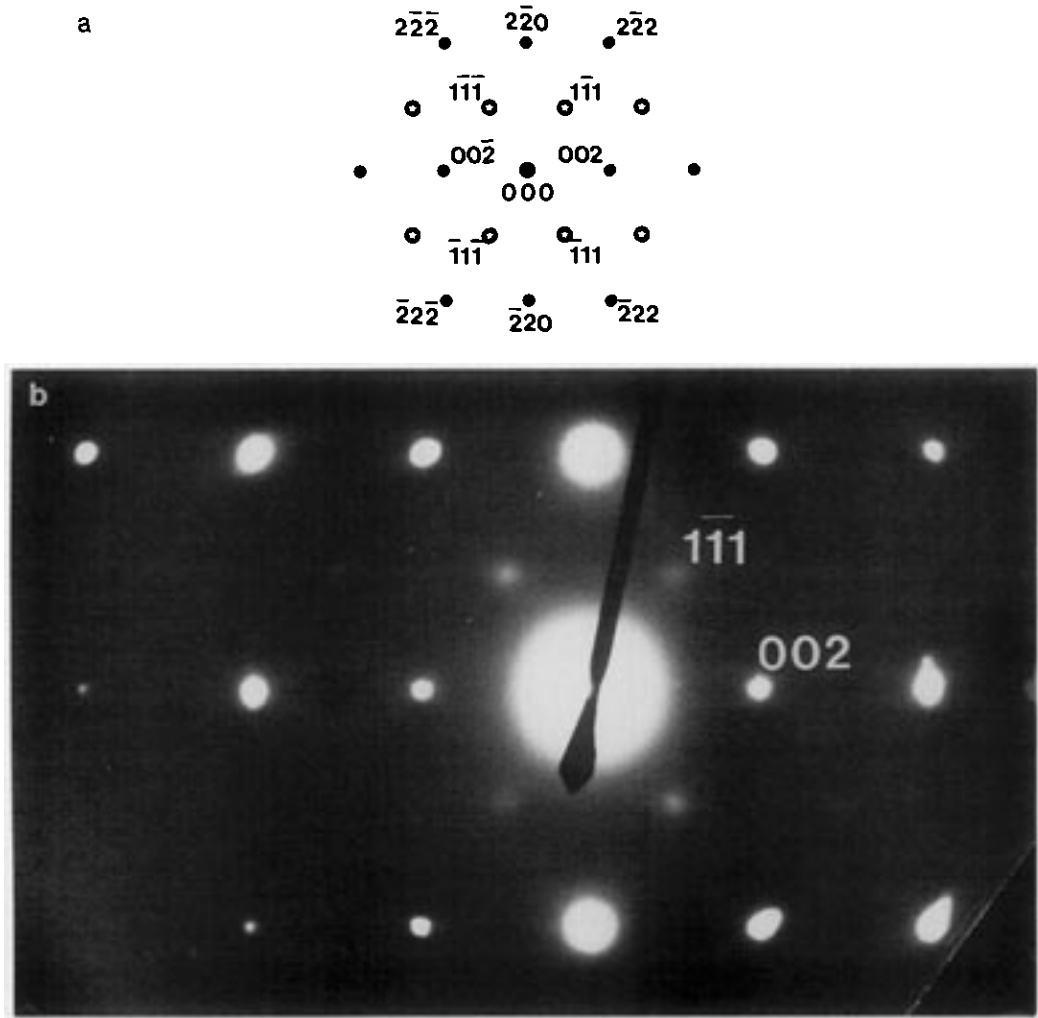
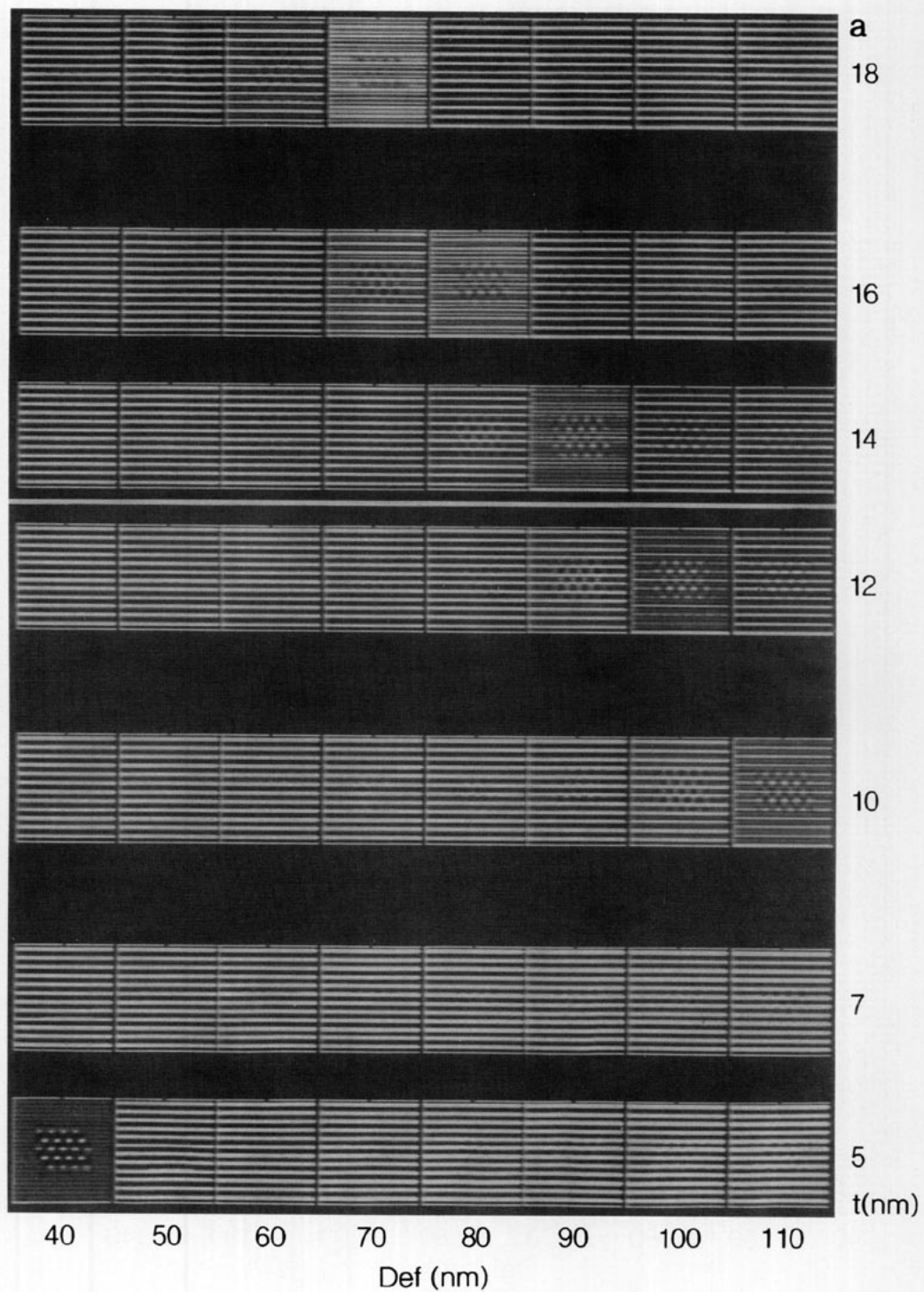


FIG. 3. Diffraction pattern along the [110] direction: (a) schematic drawing, (b) experimental result.

passage of the electrons through the sample: since we treat a nonperiodic object, we had to enclose it in a large cell (periodization). For the larger inclusions, the dimensions of this pseudoperiod were chosen as  $A = 4.884$  nm and  $B = 4.605$  nm, with a  $256 \times 256$  sampling, giving 0.019 nm per pixel. The crystalline potential was then calculated

from its Fourier coefficients,  $V_g$ , with  $g$  of up to  $26 \text{ nm}^{-1}$ . The thickness of a slice was 0.2 nm. For the smaller inclusion the dimensions of the pseudoperiod were  $A = 2.424$  nm and  $B = 3.454$  nm, with a sampling of 0.013 nm per pixel. The Fourier coefficients of the potential were then calculated up to  $36.8 \text{ nm}^{-1}$ . The slice thickness was

FIG. 4. Calculated focus series images for an ordered inclusion in a disordered matrix: (a) a 2.2-nm-thick inclusion at the top of the matrix; (b) a 2.2-nm-thick inclusion inside the matrix; (c) a 3-nm-thick inclusion in the middle of the matrix. The lateral size for the inclusion is always  $2.2 \times 1.6$  nm.



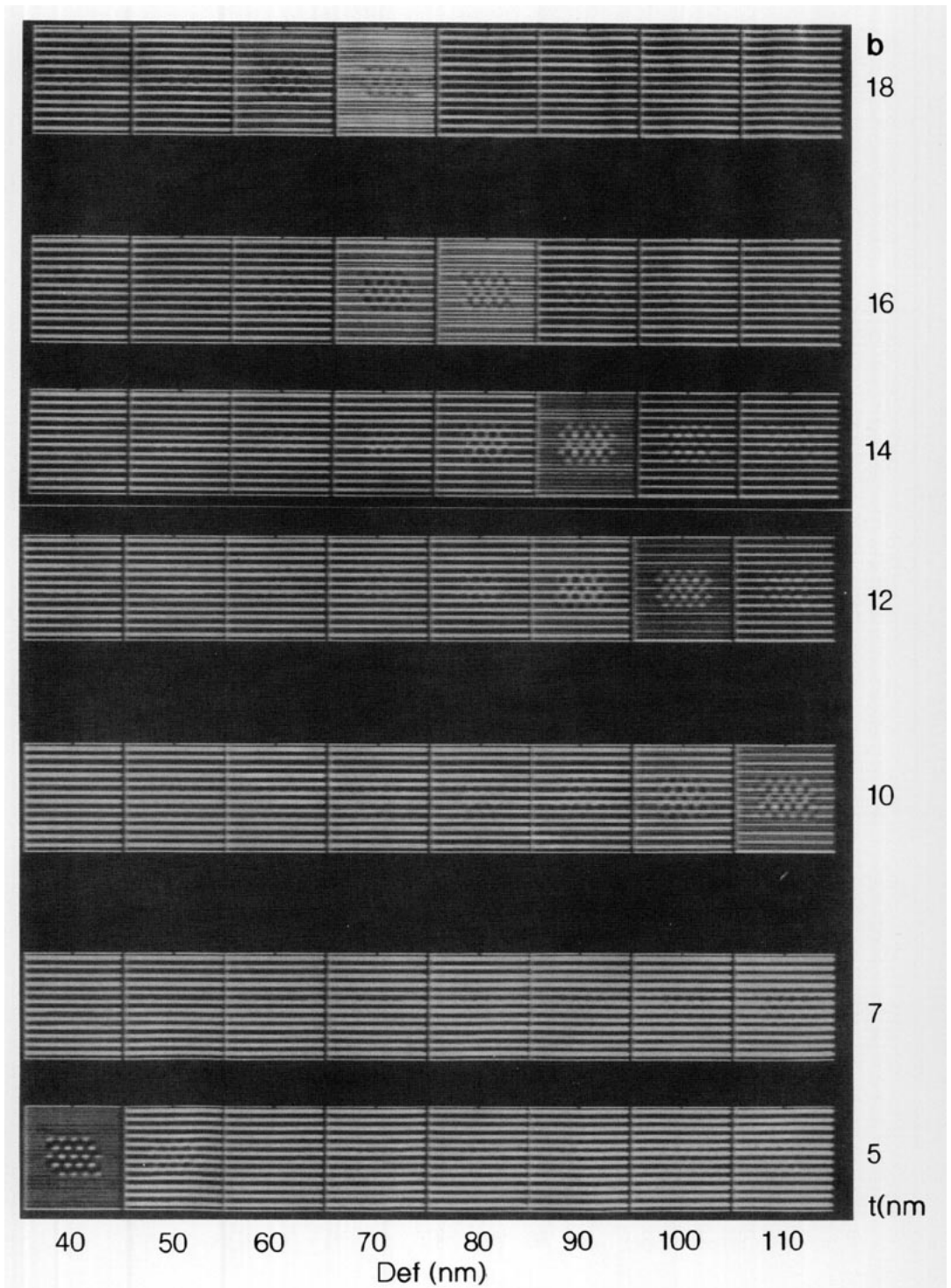


FIG. 4—Continued

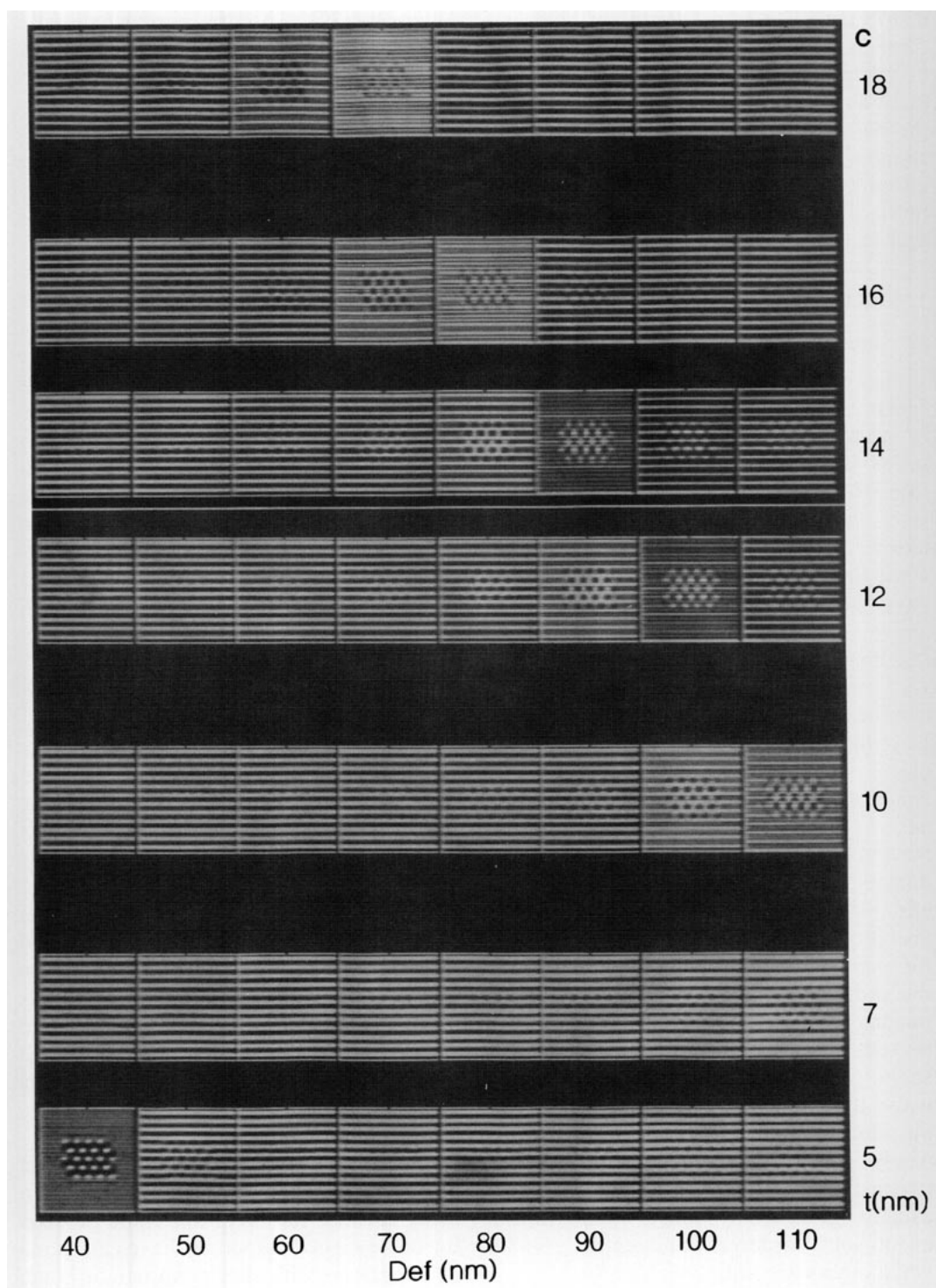


FIG. 4—Continued

0.2878 nm. The transmission of electrons through the microscope was then described taking into account the spherical and chromatic aberrations, the beam divergence, and the defocus. An objective aperture corresponding to a radius of  $2.5 \text{ nm}^{-1}$  was then introduced to obtain the specified resolution, i.e. a fringe pattern for the disordered part and a spot pattern for the ordered one.

### 3. Results

#### (a) *Specimens with Constant Thickness*

Figure 4 shows the computed images for specimens having total thickness ranging from 5 to 18 nm. For each specimen, a focus series was calculated for defoci varying from 0 to  $-110 \text{ nm}$ . Only part of it is shown, since the images repeat themselves regularly. We have studied only small defoci, since the reticular distances to be imaged have been chosen rather large as explained above. The first result in these figures is that the visibility of the ordered phase varies very rapidly with defocus and specimen thickness: though the ordered domain always has the same lateral size for each figure, it is only seen under very well defined conditions. For example, for a total thickness of 5 nm, whatever the position and the thickness (2.2 or 3 nm) of the ordered domain, it is only apparent for a small defocus ( $-40 \text{ nm}$ ). For larger thicknesses, the visibility is much improved by defocussing: for example, a defocus of  $-100 \text{ nm}$  reveals the ordered domain for a total thickness ranging from 10 to 14 nm. This is to be expected, since different thicknesses correspond to different phases for the outgoing wave: this can be compensated by the phase introduced through the defocus. Unfortunately, while for a given image the defocus is constant, the thickness of the specimen usually varies from point to point. In this event some ordered domains are visible while others are not.

When the inclusion is seen, the size of the ordered domains correspond well to our model, as expected. We assumed that the

boundaries of the ordered part were parallel to the electron beam. Then, since there are no Fresnel fringes (the disordered and ordered parts having the same mean inner potential), the images of the ordered domains have sizes nearly the same as the projection of the real object, at least for the defoci that are used. Only some effects at the edges can be seen.

Finally, we have compared the images obtained for different positions or thicknesses of the ordered domain in the disordered matrix: in Fig. 4a, the ordered part is at the top of the sample while in Figure 4b it is inside the matrix. One can see very few differences, and only in the contrast—a very difficult feature for an experimentalist to appreciate! Also, for a thicker ordered domain (Figs. 4b and 4c correspond to ordered thicknesses of 2.2 and 3 nm, all other parameters being equal), one can only say that the visibility is better, as expected. However, the ordered domain remains invisible under many experimental conditions.

#### (b) *Thin Specimens with Varying Thickness*

Here we consider a unit-cell specimen with varying thickness. Figure 5 shows the results when the small ordered inclusion is at the top of the disordered matrix: for very small thicknesses a neat pattern composed of only two or three points can be seen. This may indicate the presence of the ordered inclusion but does not provide an accurate idea of its size. When the matrix thickness increases, the inclusion becomes difficult to see except for some defoci where the (002) fringe pattern is very weak. For these defoci an artefact showing a half period appears, corresponding to a square term in the observed intensity; this experimental artefact makes these defoci easy to recognize. To ascertain that the inclusion could be seen for these special defoci, we have calculated a focus series with smaller variations in the defocus change. These are shown in Fig. 6, where one can see the fringe pattern with half the period of the (002) pattern. How-



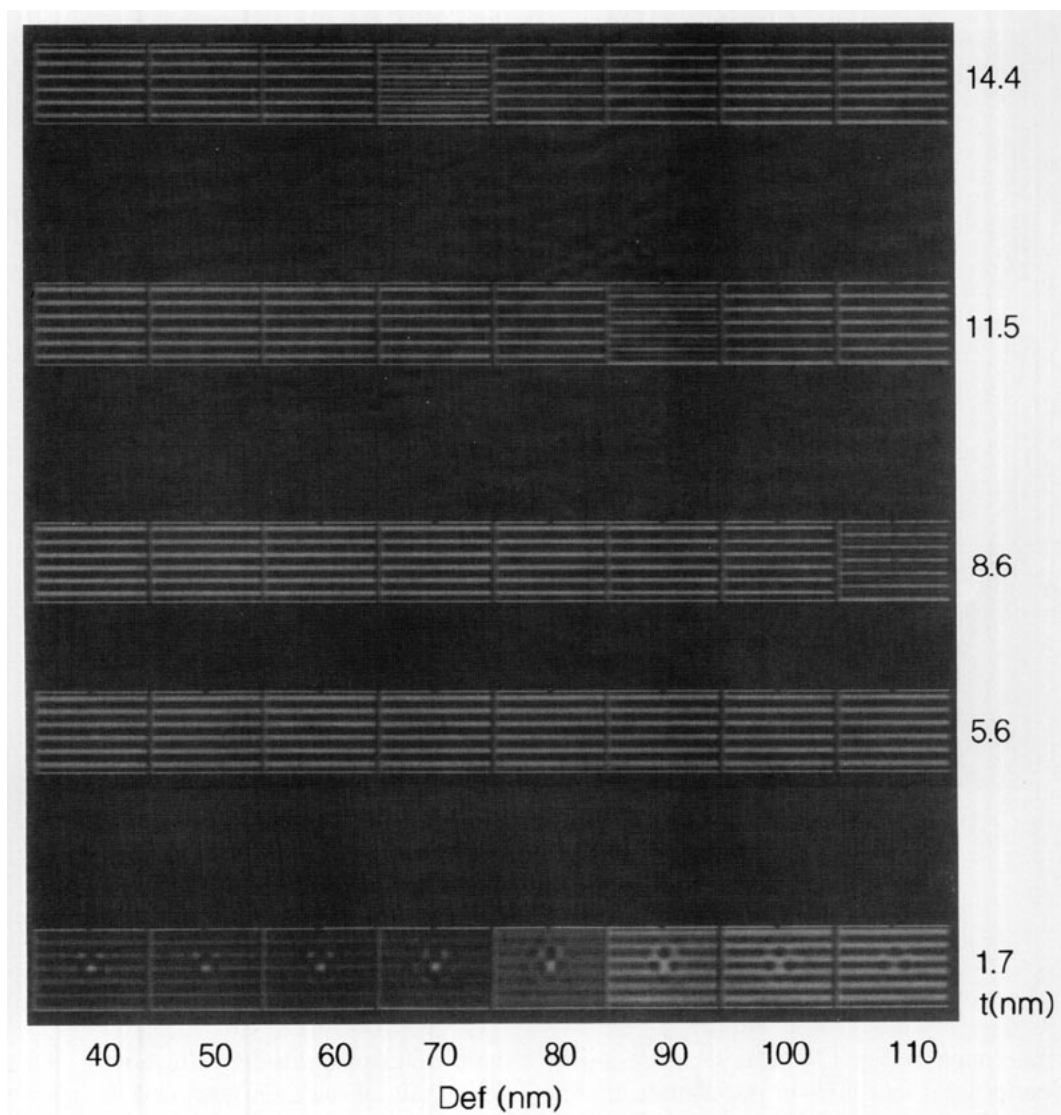


FIG. 5. Calculated focus series images for a one cell ordered inclusion at the top of the disordered matrix.

ever, for large thicknesses, the inclusion can only vaguely be observed. For smaller thicknesses (5.6 nm) the inclusion is well seen.

We have also calculated the images for different positions of the inclusion in the matrix; as the results are the same as before (inclusions are only visible for very exact defocus values different from the ones calculated above). Hence we do not show all the calculated images.

#### 4. Conclusion

This study shows that ordered domains are visible in electron microscopy structure images, using only the largest reticular distances (0.400 nm for the (200) reflection, which appears for both ordered and disordered parts, and 0.433 nm for the (111) reflections, only allowed for the ordered part). One can get some idea about their size, if they are not too small. In particular, the

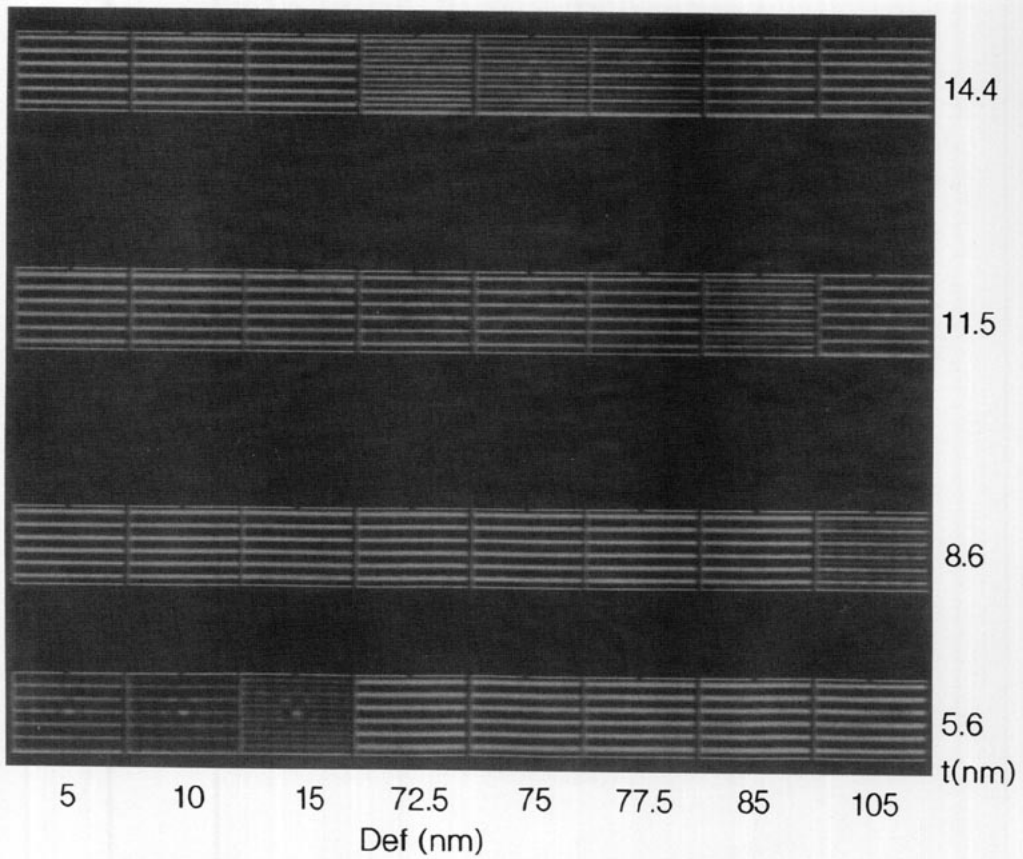


FIG. 6. Same as 4 but for very special values of the defocus, showing the precise conditions where the inclusion is slightly visible.

areas seen in Fig. 1, where there are only a few points, can now be safely interpreted as ordered domains composed of one or two cells.

However, one cannot deduce from these images the proportion of ordered domains: the existence of "spots" in the image does indicate the existence of an ordered domain but the opposite, i.e., an image with only fringes in it, does not mean that no ordered material exists in the specimen. One must record a whole focus series to be sure to include all ordered domains above a lateral size of about 2 nm. This is a rather fastidious process, but provides the only means to ascertain the proportion of ordered domains in the sample under consideration. For very

small inclusions, this depends mostly on the orientation of the inclusion, and the matrix thickness has to remain rather weak.

Hence, high resolution imaging, if correctly used, will be useful not only to reveal the existence of very small (a few cells) ordered domains in a disordered matrix, but also to obtain statistics on the ratio of ordered to disordered oxides.

### References

1. C. G. F. STENGER, F. L. SCHOLTEN, AND A. J. BURGRAAF, *Solid State Commun.* **32**, 989 (1979).
2. C. G. F. STENGER AND A. J. BURGRAAF, *Phys. Status Solidi (a)* **61**, 653 (1980).
3. N. SETTER AND L. E. CROSS, *J. Crystal Growth* **50**, 555 (1980).

4. N. SETTER AND L. E. CROSS, *J. Appl. Phys.* **51**, 4356 (1980).
5. G. A. SMOLENSKII, *Soviet Phys. Solid State* **1**, 150 (1959).
6. C. F. STENGER AND A. J. BURGGRAAF, *Phys. Status Solidi (a)* **61**, 275 (1980).
7. M. P. HARMER, A. BHALLA, B. FOX, AND L. E. CROSS, *Mater. Lett.* **2**, 278 (1984).
8. C. A. RANDALL, D. J. BARBER, R. W. WHATMORE, AND P. GROVES, *J. Mater. Sci.* **21**, 4456 (1986).
9. F. S. GALASSO, "Structure, Properties and Preparation of Perovskite-Type Compounds," Pergamon, Paris (1969).
10. N. SETTER AND L. E. CROSS, *J. Mater. Sci.* **15**, 2478 (1980).
11. H. B. KRAUSE, J. M. COWLEY, AND J. WHEATLEY, *Acta Cryst. Sect. A* **35**, 1015 (1979).
12. H. M. CHAN, M. P. HARMER, A. BHALLA, AND L. E. CROSS, *Jpn. J. Appl. Phys.* **24**, 550 (1985).
13. M. TANAKA AND G. HONJO, *J. Phys. Soc. Jpn.* **19**, 954 (1964).
14. Y. H. HU, H. M. CHAN, Z. X. WEN, AND M. P. HARMER, *J. Am. Ceram. Soc.* **69**, 594 (1986).
15. Z. C. KHANG, C. CARANONI, I. SINY, G. NIHOUL, AND C. BOULESTEIX, *J. Solid State Chem.* **87**, 308 (1990).
16. C. CARANONI, P. LAMPIN, I. SINY, J. G. ZHENG, Q. LI, Z. C. KANG, AND C. BOULESTEIX, *Phys. Status Solidi (a)* **130**, 25 (1992).
17. J. M. COWLEY, "Diffraction Physics," North Holland, Amsterdam (1975).